RSC Advances

ROYAL SOCIETY OF CHEMISTRY

www.rsc.org/advances

Journal Name

ARTICLE

Preferential <220> Crystalline Growth in Nanocrystalline Silicon Films from 27.12 MHz SiH_4 Plasma for Applications in Solar Cells

Received 00th January 20xx,
Accepted 00th January 20xx

DOI: 10.1039/x0xx00000x

www.rsc.org/

Praloy Mondal and Debajyoti Das*

It has been experimentally demonstrated that the silicon nano-crystallites (Si-ncs) are generally of <111> crystallographic orientation from random nucleation, associated to highly defective poly-hydride network at the grain-boundary; while the ultra-nanocrystallites preferably harvest a <220> alignment due to the thermodynamically preferred grain growth with concomitant mono-hydride bonding at the boundary. Using an excitation frequency (27.12 MHz) higher than the conventional frequency of 13.56 MHz, and its stimulus impact in terms of larger ion flux densities with the reduced peak ion-energy in the plasma and its associated ability to efficiently generate atomic hydrogen, nanocrystalline silicon (nc-Si) films are produced. The nc-Si:H films grown at elevated pressure demonstrate enhanced growth rate, lesser hydrogen content, lower microstructure factor, preferred <220> crystallographic orientation and possess significant fraction of ultra-nanocrystalline component in the Si-network, along with a higher intensity of mono-hydride bonding at the grain boundary by bond-centered Si–H–Si mode in platelet-like configuration. The material prepared at a low power and low temperature is extremely suitable, in every aspect, for efficient application in the fabrication of nc-Si *p-i-n* solar cells.

Introduction:

Hydrogenated nanocrystalline silicon (nc-Si:H) deposited by plasma enhanced CVD (PECVD) is a much-admired material for thin film devices e.g., solar cells, thin film transistor (TFT), etc.[1–7] Over the past few decades capacitively coupled systems (CC-PECVD) powered by radiofrequency (RF) have been widely used in thin film industries due to its associated high deposition rate and good material quality.[8–10] For further enhancing the growth rate and improving the quality very high-frequency (VHF) source are being used in recent times.[11–14] In view of its successful integration in multilayered device structure and in order to make various substrates usable for manufacturing of devices, lowering of the deposition temperature for the growth of device grade nc-Si:H network is one of the pressing agenda in the use of high frequency plasma. Regarding material issues, it has been identified that the opto-electronic devices made from films with Si-ncs having dominant <220> crystallographic orientation demonstrate better performance because of the relatively improved electronic properties of such materials. In particular, best values of open-circuit voltage (V_{OC}) in silicon solar cells identifies low recombination losses in <220> textures.[15–17]

The present work deals on exploring the influence of the higher excitation frequency (27.12 MHz), compared to the conventional frequency of 13.56 MHz, in preferable harvesting of thermodynamically superior <220> aligned crystallographic planes in nc-Si growth even at a low substrate temperature, utilizing its associated larger ion flux densities along with the reduced peak ion-energy in the plasma and its corresponding ability to efficiently generate atomic hydrogen. Spectroscopic analysis has been performed in identifying specific hydrogen bonding configurations in relation to the growth of silicon ultra-nanocrystallites (unc-Si) and the <220> crystallographic orientation.

Experimental:

The nc-Si:H films of thickness ~ 400 nm were prepared by a conventional capacitively coupled RF plasma reactor with excitation frequency 27.12 MHz, keeping the hydrogen dilution (H_2/SiH_4) fixed at 98%. Films were deposited on Corning® Eagle2000™ glass and silicon <100> wafer substrates optimizing the gas pressure within 1 to 8 Torr, while the substrate

Nano-Science Group, Energy Research Unit,
Indian Association for the Cultivation of Science,
Jadavpur, Kolkata – 700 032, India.
*E-mail (D. Das): erdd@iacs.res.in ; Fax: +91(33)24732805

temperature (Ts) was fixed at 180 ºC and the RF power applied between the electrodes was kept constant at 40 W. The deposition system with a load-lock chamber was maintained at an ultra-high vacuum in the order of 10^{-7} Torr, which provided an almost contamination-free environment for the film deposition. The samples were characterized by X-ray diffraction analysis, carried out using a conventional Cu-K_α X-ray radiation (λ ~1.5418 Å) source and Bragg diffraction setup (Seifert 3000P). Raman spectra of the samples were taken from a Renishaw in Via Raman spectroscope with an excitation wavelength of 514 nm from an air-cooled Ar^+ laser source, at a power density of ~2 mW cm^{-2}. The silicon hydrogen bonding structural was investigated using Fourier transform infrared (FTIR) spectrophotometer (Nicolet Magna-IR 750) with films deposited on polished surface of single crystal Si wafers.

Results:

Deposition rate:

Fig.1 shows the variation of the film deposition rate (R_d) that increases, in general, with pressure from 9 nm/min at p= 1 Torr to 35 nm/min at p= 8 Torr. Careful observation identifies two distinct natures of variation of R_d. The deposition rate increased with almost similar slope in the low pressure (1–3 Torr) and high pressure (6–8 Torr) regions, however, R_d increased with a considerably high slop in the medium pressure region around 3 < p (Torr) < 6, signifying a radically different growth process in effect.

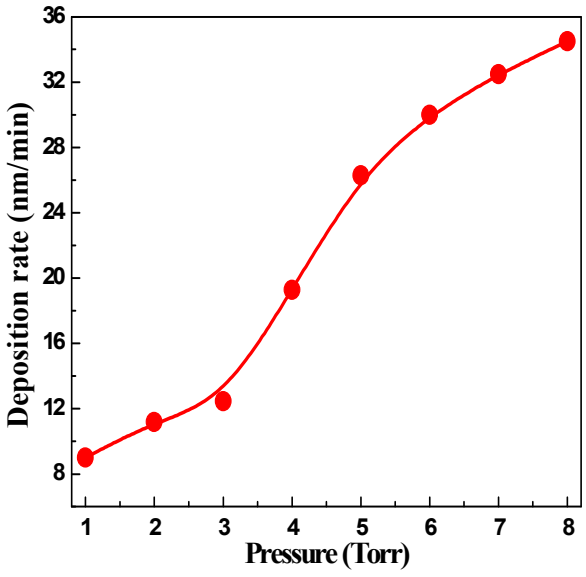

Fig. 1. Variation of the deposition rate of nanocrystalline silicon thin films on glass substrates, at different gas pressures (p).

X-ray diffraction:

The crystallinity in the Si:H network was investigated by x-ray diffraction studies. The XRD spectra of nc-Si:H films, prepared at different deposition pressures, shown in Fig.2, exhibit three dominant peaks corresponding to the <111>, <220> and <311> crystallographic orientations of c-Si, identified at 2θ =28.3°, 47.2° and 56.2°, respectively. It was previously suggested that the growth along the <220> direction is thermodynamically preferred and the grains with <220> planes are formed at elevated temperature and high pressure, while the <111> peak arises due to random nucleation.[15,18,19] In order to understand the proportional strength of specific crystallographic alignment of the nc-Si:H network, the orientation factor (Q) is defined as:

$$Q = I_{<220>} / I_{<111>},$$

where $I_{<111>}$ and $I_{<220>}$ represent the intensities of the <111> and <220> diffraction peaks, respectively. In case of silicon powder, the normalized peak intensities of the <111>, <220> and <311> directions hold an inter relation as, $I_{<111>} : I_{<220>} : I_{<311>} = 100 : 55 : 30$, according to the database of powder diffraction files JCPDS-[27-1402]. Therefore, Q= 0.55 is a critical value of the orientation factor in order to determine the preferred <220> crystallographic alignment of the nc-Si:H network. The ratio of $I_{<220>} / I_{<111>}$ is evaluated for this set of films and is shown at the inset of Fig. 2 which demonstrates that $I_{<220>} / I_{<111>}$ systematically increases with increasing gas pressure and attains the maximum magnitude of ~0.97, i.e., both the components contribute nearly equally towards crystallinity, at a gas pressure of 7 Torr.

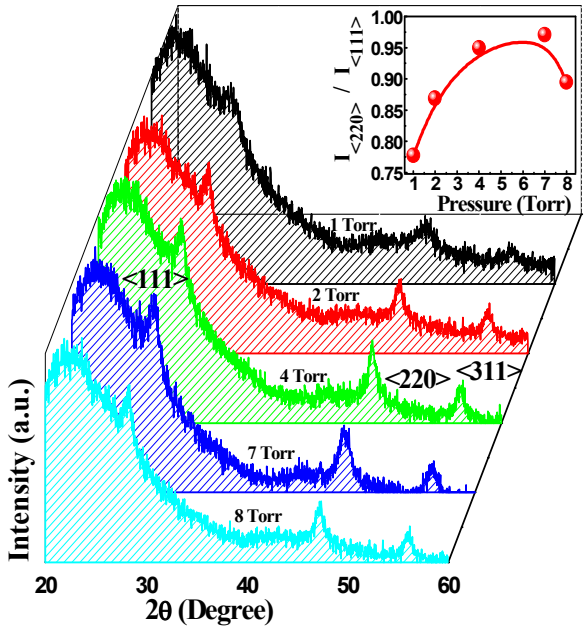

Fig. 2. XRD spectra of the Silicon films prepared at different pressures. The inset represents the change in the ratio of <220> to <111> peak intensities, $I_{<220>} / I_{<111>}$, with increasing pressure.

The ratio, however, decreases on further increase in pressure, attaining ~0.89 at 8 Torr. The preferential growth of the nc-Si grains along the <220> longitudinal direction facilitates the charge carriers to conduct perpendicular to the substrate in stacked layer devices e.g., in the nc-Si solar cells and interact with fewer grain boundaries than they do for <111>

oriented grains, while the a-Si:H component further helps to efficiently passivate the grain surface. The combination of these two phenomena serves to reduce bulk recombination and field losses and thereby, in general, increases the open-circuit voltage (V_{OC}) and fill factor (FF) of the nc-Si solar cell.[15,16,17] In the present investigation, nc-Si:H films having the preferred <220> orientation of strength, Q ~0.97 is formed at p= 7 Torr, at a low substrate temperature (180 ºC) compatible to the fabrication of solar cells.

The average grain size (D) of the nanocrystallites has been estimated from the FWHM (β) of each diffraction peak in the XRD spectra, using Scherer's formula:

$$D = 0.9\lambda/\beta cos\theta,$$

that shows a close resemblance in its nature of variation with increasing pressure along different crystallographic orientations, as shown in Fig.3. A maximum grain size of the Si-ncs ~9.5 nm along <111> direction and ~11 nm along <220> direction has been obtained.

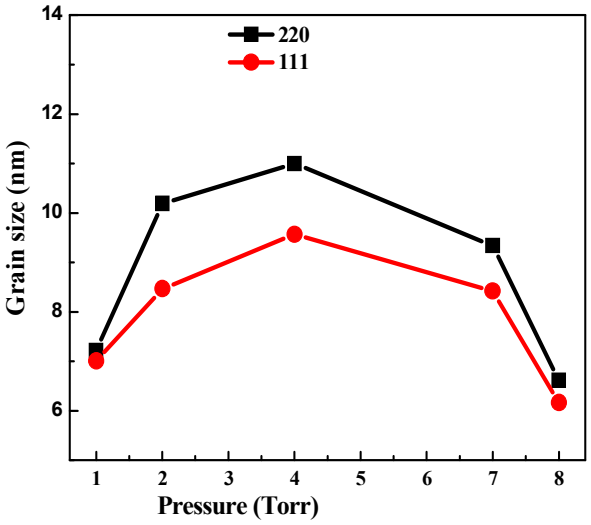

Fig.3. The variation in grain size of silicon nanocrystals with pressure.

Raman spectroscopy:

The Raman spectrum for the films prepared at different gas pressures has been presented in Fig. 4. Each Raman spectrum can be deconvoluted into three Gaussian components; the component on the higher frequency side (at around 515 cm^{-1}) represents the nanocrystalline part of the material and the lower frequency component (at ~480 cm^{-1}) arises from the amorphous part, whereas the intermediate one (at ≤ 510 cm^{-1}) corresponds to the ultra-nanocrystalline and/or the grain boundary component. The typical deconvoluted satellite components for the film prepared at p= 7 Torr has been included in Fig. 4. Careful observation on the magnified view of the Raman peaks, shown at the inset in Fig.4, clearly demonstrates a gross shift in the peak positions which is a consequence of the changes in the average size of the nanocrystallites in the network as an effect of changes in the gas pressure during growth.

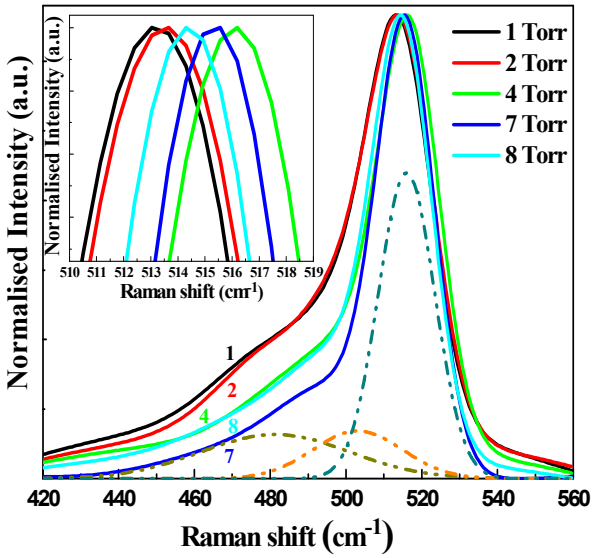

Fig. 4. Normalized Raman spectra of silicon thin films prepared at different pressures (p). The gradual shifting of peak position is observable from the magnified view in the inset.

The gross crystalline volume fraction X_C in the films can be calculated using the following equation:[20,21]

$$X_C = \frac{(I_{520}+I_{510})}{(I_{520}+I_{510}+I_{480})}$$

where I_i is the area under the Gaussian centered at i and (I_{520} + I_{510} + I_{480}) is the total integrated intensity. After deconvolution of each individual spectrum the gross crystalline volume fractions have been estimated and are shown in Fig. 5, which reveals that the X_C increases systematically from 72 % at 1 Torr to 87 % at 4 Torr and then starts gradually decreasing on further increase in pressure, attaining a magnitude of 74 % at 8 Torr.

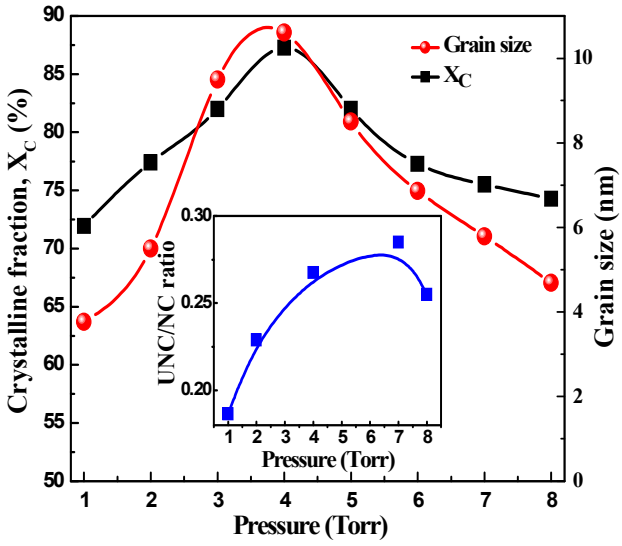

Fig. 5. The crystalline volume fraction (as estimated from Raman spectroscopy), and the variations of the mean size of Si film at different p. Inset shows the variation of UNC/NC ratio with pressure.

The average grain size has been estimated from first order Raman spectra using the following equation.[22,23]

$$(\omega_L - \omega_0)^2 + (\frac{\Gamma_0}{2})^2 \cong (\frac{1}{3L}).e^{-(\pi^2)}$$

where ω_L is the frequency of the crystalline like mode for a particle of size L and Γ_0 is the natural line width (inversely proportional to the intrinsic phonon lifetime). In case of crystalline silicon the value of ω_L and Γ_0 are 520 and 3.5 cm^{-1} respectively. The nanocrystallites attain a maximum size of ~10.6 nm at an optimum pressure of 4 Torr, while the size of the nanocrystals is miniaturized on both sides of the pressure variation. The nature of variation of the size of the nanocrystals resembles with the variation of gross crystalline volume fraction in the Si-network, X_C, as shown in Fig. 5.

It is interesting to note that the relative population of the ultra-nanocrystalline fraction (X_{unc}) to the nano-crystalline component (X_{nc}) has been found to increase monotonically with increasing gas pressure up to p=7 Torr above which it reduced in magnitude, as shown in the inset of Fig. 5. Accordingly, it is demonstrated that during increase in the gas pressure in the plasma, the material attains the maximum crystallinity corresponding to possessing the largest grain-size of the nanocrystallites with simultaneous high magnitude of X_{unc} / X_{nc} at p= 4 Torr, however, on further increase in pressure the gross crystalline volume fraction (X_C) reduces with simultaneous lowering in the size of the nanocrystals, although the ultra-nanocrystalline component keeps on preferentially populating in the network for certain extent.

FTIR study:

In order to understand the bonding structures between silicon and hydrogen in the network, infrared absorption studies have been performed with samples on Si-wafers. Fig. 6 shows the typical absorption coefficient spectra of the films prepared at different pressures in the region around 550-750 cm^{-1}. In case of amorphous silicon network the absorption band within the range (550-750) cm^{-1} usually contains the exclusive contribution of only the Si–H wagging bonds with its characteristic peak at around 640 cm^{-1}. However, for the present highly nanocrystalline silicon films the band in the region of 550-750 cm^{-1} splits into two well-resolved peaks centered at around 630 and 690 cm^{-1}, the corresponding bands are associated to the Si–H wagging and SiH_n (n≥2) rocking vibrational modes, respectively. With increase in pressure from 1 Torr to 4 Torr, the increasing crystallization in the network could be closely correlated to the increasing relative strength of the poly-hydride component, along with the reduced overall intensity of the absorption band signifying reduced hydrogenation of the network. The bonded hydrogen content (C_H) in the films has been estimated from the Si–H wagging mode vibrational component of the absorption band at 630 cm^{-1} as

$$C_H = (A_\omega/N_{Si})\int \alpha d\omega/\omega \times 100 \text{ at.\%},$$

where A_ω= 1.6 × 10^{19} cm^{-2} is the corresponding oscillator strength and N_{Si} = 5 × 10^{22} cm^{-3} is the atomic density of crystalline silicon.[24,25]

A variation of bonded hydrogen content from 10 % to 4 % with increase in pressure from 1 Torr to 8 Torr has been shown in Fig.7. It is evident from the figure that C_H changes only marginally for an initial increase in p from 1 to 3 Torr, beyond which C_H continuously reduced on increase in p. However, a relatively sharp reduction in C_H has been markedly noted for a change in p from 3 to 4 Torr, corresponding to the attainment of the highest crystallinity in the network.

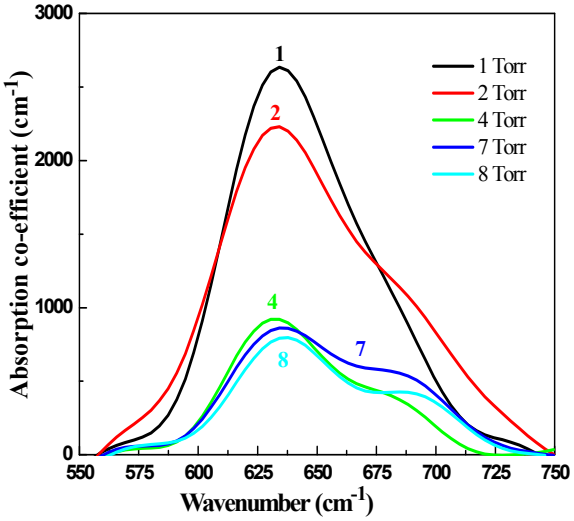

Fig. 6. Wagging mode IR absorption spectrum in the wavenumber range 550–750 cm^{-1}.

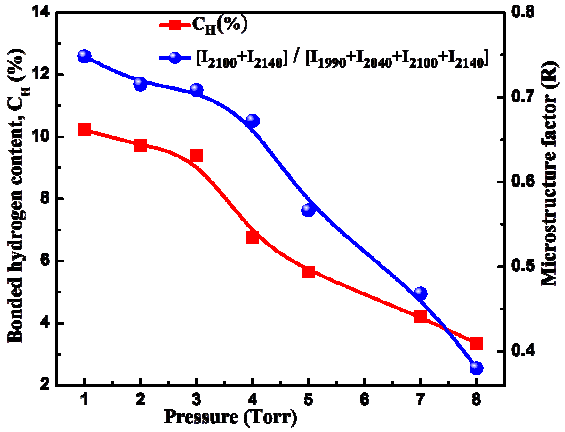

Fig. 7. Variations in the bonded hydrogen content and the microstructure factor of the nc-Si films prepared at different pressures

The absorption coefficient in the range 810 - 925 cm^{-1}, shown in Fig. 8, consists of two separate bands at 850 and 900 cm^{-1}, characteristic of bending vibrational modes of poly-hydride $(Si-H_2)_n$ complexes (isolated or coupled) and di-hydride $Si–H_2$, respectively.[26] It can be inferred from the result that in course of reduced hydrogenation in the network at higher pressure the isolated di-hydrides of silicon, $Si-H_2$, are preferentially accumulated in the form of clusters of $(Si-H_2)_n$.

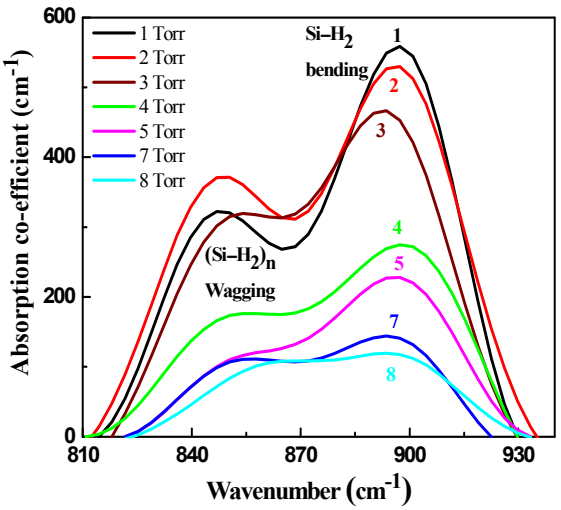

Fig. 8. IR absorption spectrum in the wavenumber range 810-925 cm^{-1}.

In addition, a considerable change in the shape and intensity of the absorption band at 1900–2220 cm^{-1} has been observed, as shown in Fig. 9. The stretching mode absorption band was contributed by its i) 1990 cm^{-1} component demonstrating the mono-hydride SiH configurations in the bonding structure, ii) a bond-centered hydrogen, Si–H–Si, identified as hydrides in a platelet-like configuration by the corresponding absorption band around 2040–2050 cm^{-1}, iii) a di-hydride Si–H_2 and poly-hydride $(Si-H_2)_n$ mode near 2100–2110 cm^{-1}, and iv) a tri-hydride SiH_3 stretching mode between 2140 and 2150 cm^{-1}. It has been identified that the intensity of mono-hydride (Si–H) bond and the bond-centered hydrogen in Si–H–Si configuration increased linearly with pressure whereas the intensity of di-hydride Si–H_2 or poly-hydride$(Si-H_2)_n$ mode decreased with increasing pressure, and the tri-hydride configuration increased corresponding to the increased crystallinity with its maximum intensity at p= 4 Torr.

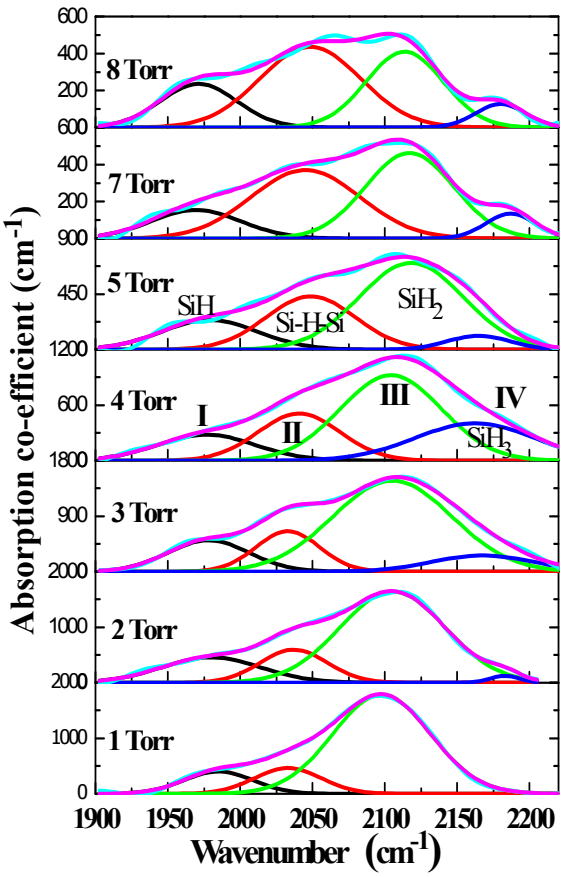

Fig. 9. Absorption coefficient spectra of deconvoluted Si–H mono-hydride and poly-hydride components and their variations with increasing pressures, indicating the formation of platelet hydride.

The microstructure factor R, defined as the fraction of poly-hydride component in the network, is presented as:

$$R = (I_{2100}+I_{2140}) /(I_{1990}+ I_{2040} + I_{2100} +I_{2140}),$$

where 'I' represents the integrated intensity under the corresponding satellite absorption bands and has been estimated for samples prepared at different pressures. The microstructure factor R has been found to gradually decrease from 0.70 to 0.40 as pressure increased from 1 Torr to 8 Torr (Fig. 7). Reducing microstructure factor, in general, corresponds to the elimination of structural imperfections in the network e.g., the presence of defects, voids and dangling bonds. Although the sample prepared at 4 Torr has the highest crystallinity but its microstructure factor is less than the relatively less crystalline film prepared at low pressure. The result happens to be opposite to the conventional H_2 diluted plasma and appears to be interesting as well.

Discussion:

It is argued that the influence of the excitation frequency on the plasma, higher than the conventional frequency of 13.56 MHz, plays a key role on the growth kinetics by allowing a highly effective dissociation of the process gas by virtue of the associated higher electron density and larger ion flux densities, leading to enhanced growth rate of the material.[11] In addition, the peak ion-energy in the plasma reduces grossly with increasing frequency, providing a much lower ion impact energy on the growing surface of the film, which could effectively reduce the surface damage and lead to superior material quality. Moreover, a sufficient amount of low-energy ion bombardment happens to be beneficial for the growth, as it may, e.g., increase the surface mobility of the radicals and desorption of reactive species.[27] The advantages of the lower electron temperature involved in the higher excitation frequency of the plasma and its ability to more efficiently generate atomic hydrogen[13,28] could be beneficial to promote the growth of nanocrystalline silicon at considerably lower levels of power and temperature, as compared with the standard glow discharge at 13.56 MHz.[29,30]

Presently, the deposition rate of the nc-Si thin films varies from 9 to 35 nm/min only, for increasing the gas pressure p from 1 to 8 Torr. This relatively low deposition rate is due to a very low magnitude of applied electrical power (40 W); however, by virtue of the relatively high frequency (27.12

MHz) of the electrical field (compared to the conventional frequency of 13.56 MHz) and its associated favorable interactions, films of ~87% crystalline volume fraction with Si-ncs of average size ~10 nm having preferred <220> crystallographic orientation has been obtained at a substrate temperature as low as ~180 ºC, compatible to the fabrication of solar cells. Films produced at higher pressure are, in general, of lesser hydrogen content, lower microstructure factor, dominantly <220>-oriented and possess significant fraction of ultra-nanocrystalline component.

It is interesting to carefully monitor on the evolution of the stretching mode of silicon-hydrogen bonding at around 2040 cm^{-1} which has been attributed to the hydrides in a platelet-like configuration that is not commonly observable in the case of nanocrystalline silicon. The hydrogen induced platelet formation in crystalline silicon (c-Si) has been reported earlier[31], along with its theoretical investigations for different structural models.[32–35] However, very few investigations have been done on the platelet formation in nc-Si material during its growth by PECVD. It was earlier reported that the peak arises due to the formation of a hydrogen-dense compact grain boundary structure with good passivation in nc-Si:H thin films.[36] According to Xu et al.[37] the process of H induced crystallization of silicon thin film by the insertion of H into the stressed Si–Si bonds leads to the formation of (a) a bond-centered hydrogen, Si–H–Si (b) an isolated silicon, H–Si– (dangling bond) and (c) a Si–Si bond with bond length close to the equilibrium c-Si bond length where the H atom is bonded to only one Si atom. The H inclusion and diffusion of H are the main reason for forming platelet-like hydrides within the nc–Si:H films.[38,39] At elevated pressure the insertion of H into the network takes place at a higher intensity of mono-hydride mode accompanied by its platelet-like configuration as observed in Fig. 9. The inclusion of H atoms into strained Si–Si bonds and its diffusion through the formation of intermediate bond–centered Si–H–Si configurations produces the platelet like hydrides.[40] The H–insertion reactions into the bond–centered location facilitate reorientation of the Si network from disorder-to-order transformation. Specifically, bond breaking and reforming reactions are facilitated by H addition, which results in elimination of strained Si–Si bonds and concerted atomic rearrangements. So the platelet like hydrides helps to grow an ordered and compact film even at higher pressure.

Evolution of the 2050 cm^{-1} band, characteristic of polymorphous silicon films, corresponds to an elevated flux of clusters to the substrate, before the onset of powder formation.[41] Formation of enhanced platelet hydrides lead to increased deposition rate of the films from typically 9 nm/min to 36 nm/min with increase in pressure from 1 Torr to 8 Torr, along with a simultaneous improvement in the order of the material,[42] particularly in terms of increasing preferential growth towards <220> crystallographic orientation that may allow to increase the efficiency and the stability of p-i-n solar cells.[43]

The explicit structural morphology of the films is determined by the crystalline volume fraction, the grain size and the specific crystallographic orientations which altogether are governed by the nature of the growth precursors involved in the formation of the network on the substrate after their generation in the plasma, and the interactions with the energetic species e.g., atomic-H, excited states of Ar (Ar*) or He (He*) and ions of the plasma with the growing surface of the solid silicon matrix.[5,44,45] It is believed that $Si–H_3$ is the main precursor responsible for the film growth in a silane–hydrogen gas mixture while other lower hydride precursors like $Si–H_x$ ($1 \leq x \leq 2$) and ions play crucial role to control the properties of the material, as they are more active. Comparing the gas phase diffusion length of $Si–H_3$ and $Si–H_x$ ($1 \leq x \leq 2$), it is accepted that the lifetime of $Si–H_x$ ($1 \leq x \leq 2$) is shorter than $Si–H_3$ and this shorter lifetime conveys their reduced diffusion length at the absorption surface on the growing network. At an elevated gas pressure the number density of lower hydrides of silicon, the higher reactive SiH_x ($x<3$) radicals and ions increases in the plasma, that in general helps increasing the growth rate of the material. However, a critical balance of available SiH_3 precursors to its lower hydride components and an efficient out diffusion of bonded H from the network promotes the highest crystallinity with largest grain size. On further rise in pressure, lowering in crystallinity with reduced grain size are the obvious consequences of increasing growth rate; while the subsequent continuous lowering in the microstructure factor could be assigned to the increasing ultra-nanocrystalline fraction (UNC/NC) of overall crystallinity in the network which is markedly different from the usual observations available in the literature. The significance of ultra-nanocrystallinity has been further probed by monitoring its relevance in controlling the orientation factor $Q = I_{<220>} / I_{<111>}$, demonstrated by the one-to-one correspondence with their preferential growth, as shown in Fig. 10.

From the experimental evidences it could be inferred that the nano-crystallites, in general, are of <111> crystallographic orientation and are associated to highly defective poly-hydride network at the grain-boundary; while the ultra-nanocrystallites preferably harvest a <220> alignment with concomitant mono-hydride bonding, presently, bond-centered hydrogen in a

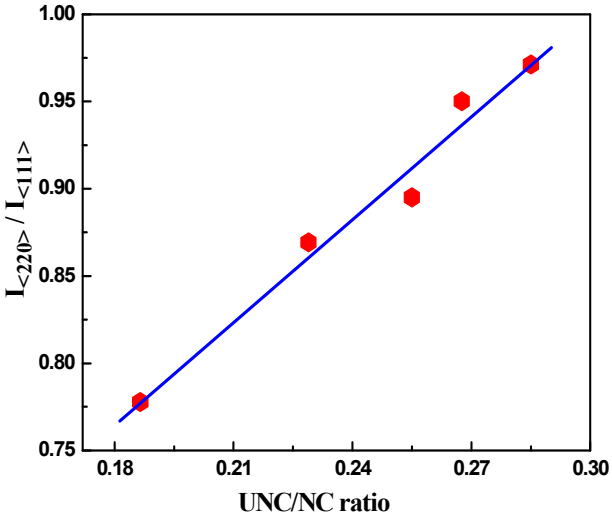

Fig. 10. Variation of $I_{<220>} / I_{<111>}$ with UNC/NC ratio of the silicon film prepared at different pressures.

platelet-like configuration at the boundary. The <111> orientation arises from random nucleation, whereas <220> due to the thermodynamically preferred grain growth with the lowest surface energy at this crystal plane.[46] In addition, crystalline grains with <220> crystallographic orientation are conducive to carrier transport and thus preferably useful in devices.[47,48]

Accordingly, formation of enhanced ultra-nanocrystalline component in the Si-network at elevated pressure, under optimized parametric condition in 27.12 MHz H_2-diluted SiH_4 plasma, promote nc-Si films of low microstructure factor with sufficiently high crystallinity (≤ 80%), small grain size (≤ 6 nm) and preferred <220> crystallographic orientation, at a low substrate temperature and an enhanced growth rate which, in every aspect, are favorable for efficient application of the material in the fabrication of nanocrystalline silicon solar cells.

Conclusion:

Nanocrystalline silicon (nc-Si) films of ~87% crystalline volume fraction with Si-ncs of average size ~10 nm and preferred <220> crystallographic orientation have been obtained at a low electrical power ~40 W, substrate temperature as low as ~180 ºC, under optimized parametric condition in 27.12 MHz H_2-diluted SiH_4 plasma. The nc-Si films produced at elevated pressure are of, in general, enhanced growth rate, lesser hydrogen content, lower microstructure factor, preferred <220> crystallographic orientation, possessing significant fraction of ultra-nanocrystalline component in the network. At elevated pressure the insertion of H into the network takes place at a higher intensity of mono-hydride bonding accompanied by its bond-centered Si–H–Si mode in platelet-like configuration.

Experimental evidences infer that the nano-crystallites are, in general, of <111> crystallographic orientationfrom random nucleation and associated to highly defective poly-hydride network at the grain-boundary; while the ultra-nanocrystallites preferably harvest a <220> alignment due to the thermodynamically preferred grain growth with concomitant mono-hydride bonding, presently, bond-centered hydrogen in a platelet-like configuration at the boundary.

Influence of the higher excitation frequency (27.12 MHz), compared to the conventional frequency of 13.56 MHz, in terms of larger ion flux densities with the reduced peak ion-energy in the plasma and its associated ability to effectively generate atomic hydrogen help producing nc-Si films having above characteristics which, in every aspect, are favorable for efficient application of the material in the fabrication of nanocrystalline silicon solar cells.

Acknowledgement:

The work has been done under nano-silicon projects funded by Department of Science and Technology (Nano-Mission Program) and Council of Scientific and Industrial Research, Government of India.

Notes and references

1 Q. Cheng, S. Xu and K.K. Ostrikov, *J. Mater. Chem*., 2009, **19**, 5134–5140.
2 J. Meier, R. Fluckiger, H. Keppner and A. Shah, *Appl. Phys. Lett*., 1994, **65**, 860–862.
3 Y. Wang, Y.P. Liu, T. Lai, H.L. Liang, Z.L. Li, Z.X. Mei, F.M. Zhang, A. Kuznetsov and X.L. Du, *RSC Adv.,* 2013, **3**, 15483-15489.
4 D. Das, *J. Phys. D: Appl. Phys.,* 2003, **36**, 2335–2346.
5 D. Das, Solid State Phenom., 1995, **44-46**, 227–258.
6 A.S. Westover, D. Freudiger, Z.S. Gani, K. Share, L. Oakes, R.E. Cartera and C.L. Pint, *Nanoscale*, 2015, **7**, 98–103.
7 X. Liu, P.R. Coxon, M. Peters, B. Hoex, J.M. Cole and D.J. Fray, *Energy Environ. Sci*., 2014, **7**, 3223–3263.
8 D. Das and A. Samanta, *Nanotechnology*, 2011, **22**, 055601.
9 T.F. Cao, H.B. Zhang, B.H. Yan and Y. Cheng, *RSC Adv*., 2013, **3**, 20157–20162.
10 T.F. Cao, H.B. Zhang, B.H. Yan, W. Lu and Y. Cheng, *RSC Adv*., 2014, **4**, 15131–15137.
11 F. Finger, U. Kroll, V. Viret, A. Shah, W. Beyer, X. M. Tang, J. Weber, A. Howling, and C. Hollenstein, *J. Appl. Phys.*, 1992, **71**, 5665-5674.
12 M. Kondo, M. Fukawa, L. Guo and A. Matsuda, *J. Non-Cryst. Solids*.,2000, **266–269**, 84–89.
13 H. Yang, C. Wu, J. Huang, R. Ding, X. Geng and S. Xiong, *Thin Solid Films*, 2005, **472**, 125– 129.
14 S. Ray and S. Mukhopadhyay; Phil. Mag., 2009, 89, 2573–2585.
15 V.L. Dalal, K. Muthukrishnan, X. Niu and D. Stieler, *J. Non-Cryst. Solids*., 2006, **352**, 892–895.
16 J.H. Werner, K. Taretto and U. Rau, *Solid State Phenom*., 2001, **80–81**, 299–304.
17 P.E. Vallat-Sauvain, A. Shah, J. Bailat, J. Poortmans and V. Arkhipov, Advances in Microcrystalline Silicon Solar Cell Technologies in Thin Film Solar Cells: Fabrication, Characterization, and Application, first ed., John Wiley and Sons, England, 2007, 13–171.
18 D. Raha and D. Das, Appl. Surf. Sci., 2013, 276, 249– 257.
19 A. Banerjee and D. Das; Appl. Surf. Sci., 2015, 330, 134–141.
20 G.Z. Yue, J.D. Lorentzen, J. Lin, D.X. Han and Q. Wang, *Appl. Phys. Lett.*, 1999, **75**, 492–494.
21 D. Das, *Thin Solid Films*, 2005, **476**, 237–245.
22 B.sain and D. Das, *Sci. Adv. Mater.,* 2013, **5**, 188–198.
23 B. Sain and D. Das, *Phys. Chem. Chem. Phys*., 2013, **15**, 3881–3888.
24 C.J. Fang, K.J. Gruntz, L. Ley, M. Cardona, F.J. Demond, G. Muller and S. Kalbitzer, *J. Non-Cryst. Solids*.,1980, **35–36**, 255–260.
25 D. Kar and D. Das, *J. Mater. Chem. A*, 2013, **1**, 14744–14753.
26 D. Das, *Solid State Commun*., 1998, **108**, 983–987.
27 M. Heintze, R. Zedlitz and G.H. Bauer, *J. Phys. D: MI. Phys.*, 1993, **26**, 17814786.
28 F. Finger, P. Hapke, M. Luysberg, R. Carius, H. Wagner and M. Scheib, *Appl. Phys. Lett*., 1994, **65**, 2588–2590.
29 S. Oda, J. Noda and M. Matsumura, *Mater. Res. Soc. Symp. Proc.,* 1988, **118**, 117.
30 K. Prasad, F. Finger, S. Dubail, A. Shah and M. Schubert, *J. Non-Cryst.Solids*., 1991, **137–138**, 681.
31 N.M. Johnson, F.A. Ponce, R.A. Street and R.J. Nemanich, *Phys. Rev. B*, 1987, **35**, 4166.
32 M. Bruel, *Electron. Lett.*,1995, **31**, 1201.
33 C.G. Van de Walle, Y. Bar-Yam and S.T. Pantelides, *Phys. Rev.Lett.*, 1998, **60**, 2761.
34 F.A. Reboredo, M. Ferconi and S.T. Pantelides, *Phys. Rev. Lett.*, 1999, **82**, 4870.

35 J. Grisolia, G.B. Assayag and A. Claverie, *Appl. Phys. Lett.*, 2000, **76**, 852.

36 S. Vignoli, R. Butte, R. Meaudre, M. Meaudre and R. Brenier, *J. Phys.:Condens. Matter*., 2003, **15**, 7185–7200.

37 L. Xu, Z.P. Li, C. Wen and W.Z. Shen, *J. Appl. Phys*., 2011, **110**, 064315.

38 S . Agarwal, B. Hoex, M.C.M. van de Sanden, D. Maroudas and E.S. Aydil, *J. Vac. Sci. Technol. B*., 2004, **22**, 2719.

39 M.S. Valipa, S. Sriraman, E.S. Aydil and D. Maroudas, *J. Appl. Phys*., 2006, **100**, 053515.

40 S. Sriraman, S. Agarwal, E.S. Aydil and D. Maroudas, *Nature*, 2002, **418**, 62–65.

41 P. Roca i Cabarrocas, *J. Non-Cryst. Solids.*, 2000, **266–269**, 31–37.

42 A. Fontcuberta i Morral and P. Roca i Cabarrocas, *J. Non-Cryst. Solids.*, 2002, **299–302**, 196–200.

43 P. Roca i Cabarrocas, P. St'ahel, S. Hamma and Y. Poissant, *Proc. 2nd World Conference on Photovoltaic Solar Energy Conversion*, Vienna, Austria, 1998, 355, J. Schmid, H.A. Ossenbrink, P. Helm, H. Ehmann and E.D. Dunlop, Report EUR 18656 EN, Joint Research Centre, European Commission.

44 M. Jana, D. Das and A.K. Barua; *Sol. Energy Mater. & Sol. Cells*, 2002, **74**, 407–413.

45 D. Das, D. Raha and K. Bhattacharya; *J. Nanosci. & Nanotech.*, 2009, **9**, 5614–5621.

46 Y. Sun, T. Miyasato and J.K. Wigmore, *Appl. Phys. Lett.*,1997, **70**, 508–510.

47 T. Kamiya, K. Nakahata, A. Miida, C.M. Fortmann and I. Shimizu, *Thin Solid Films*,1999, **337**, 18–22.

48 V.L. Dalal, K. Muthukrishnan, M. Noack and E. Schares, J. *Appl. Phys.*, 2006, **100,** 036106.